

## Structural health monitoring of turbo generator foundation

Fatemeh Sharafi \*, Reza Karami Mohammadi \*\*

### ARTICLE INFO

#### RESEARCH PAPER

#### Article history:

Received:

June 2023

Revised:

January 2024

Accepted:

May 2024

#### Keywords:

Damage detection,  
Hilbert transform,  
FE model updating,  
GA algorithm,  
Signal processing

### Abstract:

Structural health monitoring has been widely used during the past decades to evaluate the safety of structural assets, detect damage at an early stage, and prevent unexpected and costly damages. The research in this field is often concerned with bridges and buildings and little research has been conducted on structural health monitoring of power plant infrastructures such as machine foundations. The turbo generator, also referred to as the heart of the power plant, is supported by massive concrete foundations in the turbine hall of thermal power plants. Most Turbine Generator (TG) foundations in thermal power plants are at or close to their design age. The reports on structural damage in thermal power plants show that cracks are frequently observed on the beams and columns of frame-type TG foundations. It is probably the most appropriate time for developing vigorous methods for health monitoring of power plant structures to extend their reliability and life span. This paper employs the vibration-based approach for damage detection of TG foundations. Analytical mode decomposition (AMD) and experimental mode decomposition (EMD) methods are both used for modal parameter identification. A genetic algorithm is further used for finite element model updating and damage detection. The performance of the method is investigated using a 3-D finite element model of a frame-type TG foundation.

### 1. Introduction

The TG, usually referred to as the heart of the power plant, is supported by a massive foundation pedestal in the turbine hall. The TG foundation deteriorates due to normal aging, environmental factors, and natural events such as earthquakes. It is also continuously exposed to the harmonic vibration of the TG machine.

The safety and stability of the TG largely depend on its foundation safety and stability so that any failure in structural performance of the foundation may result in failures and shutdowns of turbo generator.

Some power plant structures such as cooling towers and pipe racks have been analyzed and assessed by sensor-based monitoring systems in the previous studies [1], [2].

However, little research has been conducted on monitoring and maintenance of the TG foundations. Although the TG foundations rarely collapse because of their conservative design criteria, local cracks on the beam-column elements were frequently observed during the inspection of TG foundations in some thermal power plants. Also, some research studies reported damage including cracks in TG foundations [3]. In the long run, even minor deteriorations can lead to costly damages if they remain undetected. These events may lead to unplanned shut downs, disturbance in the power generation process, and even the failure of the machine.

The fact that the dynamic properties embedded in the structure's vibration data are functions of the structure's physical characteristics, has led to the development of vibration-based structural health monitoring. Changes in physical properties of the structure such as mass, stiffness and dissipation energy cause changes in its dynamic responses and modal properties including frequency, mode shape and damping. Vibration-based methods are based on the analysis and monitoring of modal properties of the

\* M.Sc. in Earthquake Engineering, Department of Civil Engineering, KN Toosi University of Technology, Tehran, Iran.

\*\* Corresponding Author: Associate Professor, Department of Civil Engineering, KN Toosi University of Technology, Tehran, Iran.

Email: [rkarami@kntu.ac.ir](mailto:rkarami@kntu.ac.ir)

structure, and are considered global tools that assess the overall performance of the structure. Different modal properties including modal frequencies, mode shapes, modal strain energy, and others are commonly used as damage indicators for damage detection purposes [5-11]. Finite element model updating (FEMU) is a compelling vibration-based technique by which the parameters of the FE model are updated to match up the responses of the FE model with those of the real structure. Model updating upgrades the numerical model into a reasonable agreement with the real structure. Since damage changes the physical parameters of the structural system, this process could also be used for damage detection purposes by updating the dynamic parameters of the intact model (i.e., the FE model) so that the responses of the intact model match those of the damaged model.

Abdel Wahab [12] identified the damage in a simply supported beam by updating its sensitivity matrix. The sensitivity matrix was constructed using the residuals between the measured modal data and finite element modal data with respect to the unknown parameter perturbations. In this research, the modulus of elasticity of beam elements was considered as the updating parameters or unknown parameters. First, the modal frequencies and mode shape values, and then the aforementioned parameters along with the modal curvature values, were considered for the sake of residual formulation. The results showed that adding the mode shape curvature to the updating algorithm does not improve the convergence.

Yu and Yin [13] proposed a model updating technique for damage detection in frame structures. The objective function was to minimize the frequency and mode shape error vectors before and after the damage occurrence using a least-squares problem. The locations and intensities of damages in different scenarios were estimated flawlessly. The method proposed by Li and Hao [14] localized and quantified the damage induced in an experimental 7-story frame structure, using finite element model updating. The proposed method, minimized the discrepancy between the measured and the constructed acceleration time histories of the structure, based on a wavelet-domain response reconstruction method.

Recently, model updating using computational intelligence and evolutionary algorithms (EAs) has become a major focus of research. Alkayem et al. [15] provided a survey on the applications of evolutionary algorithms in model updating. They also compared the efficiency of different evolutionary algorithms including genetic algorithm (GA) and particle swarm optimization (PSO) for damage detection in the ASC-ASCE SHM benchmark building.

Cha and Buyukozturk [16] used a hybrid multi-objective genetic algorithm for damage detection in complex three-

dimensional steel structures. The main aim of the study was to detect minor damages that were undetectable by traditional methods based on modal properties.

Chen and Wang [17] compared the accuracy of EMD, filtering, and AMD methods for different vibration signals. The AMD technique proved to be much more accurate than the other methods in mode decomposition. It was capable of separating the vibration modes without distorting the time domain data and was a strong method for the decomposition of closely-spaced modes. Moreover, it was shown to have lower sensitivity to noise.

The authors later used AMD and Hilbert transform for frequency and damping identification in civil structures under ambient excitations [18]. They separated the modal vibrations using AMD, applied Hilbert transform to the first decomposed components to obtain the instantaneous phase and amplitude, and computed the modal frequencies and damping ratios from each of instantaneous properties in a 36-story building.

This study aims to fill the gap in the field of structural health monitoring of power plant structures by applying vibration-based techniques for damage detection of a typical TG foundation model.

For this purpose, Hilbert transform combined with two decomposition methods (EMD and AMD) is implemented and their reliability for damage detection of TG foundations is evaluated.

## 2. Theoretical background

### 2.1 Hilbert transform

Unlike the stationary signals where the frequency and amplitude are constant in time, the nonstationary signals have time-varying characteristics. Traditional transformations used in signal decomposition such as Fourier transform are unable to represent the changeable behavior of nonstationary signals over time. Hilbert transform was introduced by a mathematician named David Hilbert to address this problem. It can extract the instantaneous characteristics including phase, amplitude and frequency of the signals.

Hilbert Transform is a famous method in vibration analysis. It performs as a filter that shifts the signal's phases by 90 degrees ( $0.5\pi$ ) and derives the signal's instantaneous frequency, amplitude, and phase in the time domain.

Hilbert transform of the signal  $y(t)$  is defined as:

$$H[y(t)] = \tilde{y}(t) = \pi^{-1} \int_{-\infty}^{\infty} \frac{y(\tau)}{t - \tau} d\tau \quad (1)$$

Where  $\tilde{y}(t)$  is the orthogonal projection of  $y(t)$  after convolution with kernel function  $1/\pi t$ . Moreover, the

integral function is considered a Cauchy principal value since a singularity might occur at  $t = \tau$ .

The analytic signal is constructed by the signal itself, which is the real part, and its Hilbert transform, which is the imaginary part:

$$y(t) = A(t)\cos \psi(t) \quad (2)$$

$$Y(t) = y(t) + j\tilde{y}(t) = A(t)\exp[j\psi(t)] \quad (3)$$

The analytic signal in exponential form is defined as:

$$\begin{aligned} Y(t) &= |Y(t)|[\cos \psi(t) + j\sin \psi(t)] \\ &= A(t)e^{j\psi(t)} \end{aligned} \quad (4)$$

Therefore, the instantaneous amplitude, phase, and angular frequency could be obtained using equations (5) to (7), respectively [19]:

$$A(t) = |Y(t)| = \sqrt{y^2(t) + \tilde{y}^2(t)} = e^{\text{Re}[\ln Y(t)]} \quad (1)$$

$$\varphi(t) = \arctan(\tilde{y}(t)/y(t)) \quad (2)$$

$$\omega(t) = \dot{\varphi}(t) \quad (3)$$

Where  $y(t)$  and  $\tilde{y}(t)$  are the vibration signal and its Hilbert transform, respectively.  $Y(t)$  is the analytic signal form,  $A(t)$  is the amplitude signal,  $\varphi(t)$  is the instantaneous phase, and  $\omega(t)$  is the instantaneous angular frequency.

For a simple mono-component signal (e.g., the response of an SDOF system), the instantaneous frequency and amplitude are constant since the signal contains only one mode of vibration. But in most real-world vibrations, the instantaneous characteristics of the signal vary in the time domain and may also change sign when the phasor's rotation changes direction from counterclockwise to clockwise. It is generally more desirable to decompose the signal to its simple components and then use Hilbert transform for feature extraction [20].

Huang et al. [21] proposed a method for decomposing nonstationary signals to mono-components that admit well-behaved Hilbert transforms.

## 2.2 Hilbert-Huang transform

Huang et al. [21] introduced the Empirical Mode Decomposition (EMD) method, which allows a multi-component signal to be expressed as a sum of mono components, known as Intrinsic Mode Functions (IMFs). This technique was then combined with the Hilbert transform to form the Hilbert-Huang transform. The EMD method identifies the single oscillation modes of the signal through a process known as sifting. Each mode function, or IMF, represents a simple oscillatory component of the signal and is independent of other components. An IMF must meet two criteria: the number extrema and zero crossings should either be equal or differ by at most one, and at any point, the mean value of the envelope defined

by the local maxima and the envelope defined by the local minima should be zero. To obtain the intrinsic modes, the mean of the upper and lower envelopes of the signal, obtained through spline fitting, is subtracted from the signal. This process is referred to as the sifting process.

$$X(t) - X_{m1}(t) = h_1 \quad (4)$$

Where  $x(t)$  is the signal and  $X_{m1}$  is the mean of the envelopes, defined as:

$$X_{m1}(t) = \frac{X_{max} + X_{min}}{2} \quad (5)$$

This procedure is repeated until the resulting signal,  $h_1$ , satisfies the IMF conditions and thus, could be regarded as a mono-component. Otherwise, the resulting signal is treated as a new signal, and the sifting process is repeated until the IMF requirements are met:

$$h_1 - X_{m11}(t) = h_{11} \quad (6)$$

The first IMF obtained after  $k$  times repeating the sifting process is:

$$c_1(t) = h_{1k} \quad (7)$$

To extract the second IMF,  $c_1$  is subtracted from the signal, giving the residue  $r_1(t)$  as:

$$X(t) - c_1(t) = r_1(t) \quad (8)$$

The sifting process continues until the residue reaches a predefined value or becomes a monotonic function. Therefore, the primary signal is constructed by  $n$  IMFs,  $c_n$ , and the final residue:

$$X(t) = \sum c_i(t) + r_n \quad (9)$$

They also defined a stop criterion for the sifting process. In this definition, the sifting process stops when the standard deviation of the two consecutive sifting results, as defined in equation (14), gets a value between 0.2 and 0.3:

$$SD = \sum_{t=1}^T \left[ \frac{|h_{1(k-1)}(t) - h_{1k}(t)|^2}{h_{1(k-1)}^2(t)} \right] \quad (10)$$

## 2.3 Analytical mode decomposition and Hilbert transform

Chen and Wang [17] developed a new technique for signal decomposition called analytical mode decomposition (AMD) to extract mono component vibration modes from a multi component signal. In this new approach, a nonlinear and nonstationary signal,  $x(t)$ , can be expressed as a sum of  $n$  single-frequency components,  $x_k^d$  ( $k=1, 2, \dots, n$ ), with  $n$  exclusive natural frequencies. It can be defined as:

$$x(t) = \sum_{k=1}^n x_k^{(d)}(t) \quad (11)$$

Each individual signal carries a single mode of vibration which is obtained by equation (16):

$$\begin{aligned} x_1^{(d)}(t) &= S_1(t). x_2^{(d)}(t) \\ &= S_2(t) - S_1(t). x_k^{(d)}(t) \\ &= S_k(t) - S_{k-1}(t). x_n^{(d)}(t) \\ &= x(t) - S_{n-1}(t) \end{aligned} \quad (12)$$

$$\begin{aligned} S_k(t) &= \sin(\omega_{bk}t)H[x_j(t) \cos(\omega_{bk}t)] \\ &\quad - \cos(\omega_{bk}t)H[x_j(t) \sin(\omega_{bk}t)] \end{aligned} \quad (13)$$

$k = 1.2 \dots n - 1$

Where  $\omega_{bk}$  is the bisecting frequency, placed between each two natural frequencies. The  $H[]$  sign is the Hilbert transform operator. The bisecting frequencies are recommended to be the average of the two natural frequencies. However, the AMD process is insensitive to bisecting frequency selection in the range of 0.8 to 1.2 of the average frequency.

The AMD technique is applicable to both stationary and nonstationary signals. It was developed to address the challenges of previous techniques such as EMD and band-pass filtering in accurate signal decomposition of modes with overlapping frequency.

#### 2.4 Finite element model updating method

The damage detection procedure for an undamped, linear system could be explained using the system dynamic equation of motion, defined as:

$$[M][\ddot{x}] + [K][x] = 0 \quad (14)$$

Where  $[M]$  is the mass matrix;  $[K]$  is the stiffness matrix;  $[x]$  is the displacement vector. The equation (18) is solved by:

$$x(t) = \phi_i u_i(t) \quad (15)$$

$$u_i(t) = A_i \cos(\omega_i t - \theta_i) \quad (16)$$

Where  $\phi_i$ ,  $\omega_i$ ,  $u_i$ ,  $\theta_i$ , and  $A_i$  are the  $i^{\text{th}}$  mode shape, the  $i^{\text{th}}$  modal frequency, the  $i^{\text{th}}$  time variation of displacement under harmonic excitation, the  $i^{\text{th}}$  phase angle, the  $i^{\text{th}}$  constant related to the  $i^{\text{th}}$  mode shape, respectively.

Substituting the equations (19) and (20) into (18) gives the equation (21):

$$u_i(t)(-\omega_i^2[M]\phi_i + [K]\phi_i) = 0 \quad (17)$$

Equation (21) is solved through equation (22):

$$([K] - \omega_i^2[M])\phi_i = 0 \quad (18)$$

Then, it is sensible to describe the damage as a reduction in the system stiffness and insert it in the FE model updating procedure as:

$$[K]_d = [K]_u(1 - \alpha_j) \quad (19)$$

Where the subscripts d and u represent the stiffness matrices of the damaged and intact structures, respectively.  $\alpha_j$  is a scalar value representing the damage index of the  $j^{\text{th}}$  element, that is defined between 0 and 1; when  $\alpha_j$  is zero, the element is healthy and when it equals 1, the element is totally damaged.

Through FE model updating, the problem can be expressed as:

$$\begin{aligned} R_i(\alpha_1, \alpha_2, \dots, \alpha_n) &= \{[K]_d - (\omega_i^d)^2[M]\} \phi_i^d \\ r &= 1, \dots, n \end{aligned} \quad (20)$$

$$F = \sum_{i=1}^r \|R_i\|^2 \quad (21)$$

where  $R_i$ ,  $F$ ,  $r$ ,  $\omega_i^d$  are the  $i^{\text{th}}$  residual corresponding to  $i^{\text{th}}$  mode, the objective function, the number of the considered vibration modes, and the natural frequency of the  $i^{\text{th}}$  mode, respectively.

The objective function is defined as a residual between the intact and damaged structure that is minimized through optimization. Selecting appropriate updating parameters is a crucial task in the model updating procedure. A typical approach for choosing suitable parameters stems from the convention that damage can be defined as a change in the physical parameters of the structure. Material and geometrical parameters such as modulus of elasticity, density, cross-sectional area, and moment of inertia are related to the main characteristics of the structure (mass, stiffness) and can be indicators of damage. Elemental stiffness reduction is a conventional method for representing damage while protecting structural connectivity [22]. Moreover, it is desirable to keep the number of updating parameters small to reduce the computational efforts [23].

#### 2.5 Genetic algorithm

John Holland developed the genetic algorithm (GA) in the 1960s based on the principles of evolution. The GA is a mathematical model of Darwin's natural selection theory of "survival of fittest". Since then, it has been widely used in optimization problems.

This algorithm generates a random population of individuals, called the chromosomes, which represent candidate solutions to the problem. Each chromosome

contains an array of genes whose length depends on the number of problem variables. In a binary-coded GA, the genes are arrays of zeros and ones. The GA can also be real-coded, where the genes represent real numbers. In this case, the genes are defined with minimum and maximum values. Choosing the type of GA is problem-specific.

A genetic algorithm requires an objective function. The algorithm evaluates the fitness of each solution and determines the extent to which the solutions satisfy the objective function. Those chromosomes that have the highest fitness values will be selected for the next generation. In short, the higher the fitness values, the higher the probability of being chosen for the next generation. This results in removing the low-quality individuals and passing on high quality information to the next generation. However, this process causes a number of highly fit individuals to dominate the selection process. The next generations inherit the same weaknesses and strengths of the prior generations. This reduces the quality of search. To tackle the problem, the individuals undergo crossover and mutation.

The crossover operator randomly selects some individuals (called parents) to combine their information by crossing their genes at randomly chosen points, and reproduces new off-springs. The operation may be single-point, double-point or uniform crossover. The number of genes exchanged between two parents depends on the crossover probability  $\rho_c$ .

The chromosomes also undergo the mutation operator. Mutation replaces a gene from a chromosome with a randomly chosen gene from the search space. It improves the quality of the search by introducing new information and maintaining diversity. It is recommended to keep the mutation probability small.

The algorithm stops when the termination criteria are satisfied or the predefined number of iterations is completed.

### 3. Numerical modelling and model updating procedure

#### 3.1 turbo generator foundation model

The most widely adopted TG foundations in the industry are block and frame foundations [4]. Frame-type foundations consist of a top deck, a set of beam and column elements, and a base raft. These foundations are well-suited for supporting high-speed machinery. They offer numerous benefits such as space and material saving, easy access for machine inspection, and reduced susceptibility to settlement and temperature-induced cracks.

Because of the limitations in accessibility to design documents of TG foundations, the frame type foundation characterized in [4] was used in this study. It provided

sufficient information about the structure material properties, sizing, and loads. The model is simplified but an adequate representation of a typical TG foundation. The 3-D FE model was simulated using the commercial FEM software SAP2000 (Figure 1).

In this study, the foundation is assumed to be fixed at the bottom of columns. The beams and columns are modeled by frame elements, and the top deck is modeled by shell elements with shear deformations. Rigid beam elements, with Young's moduli significantly larger than those of the frame elements are modeled to connect the machine bearings to the machine center of gravity and transfer the loads from machine to the deck. Furthermore, rigid elements are used to model the beam-column joint sizes to simulate the effect of "short span and large joint size". For the ease of implementation, the soil-structure interaction is ignored. The natural frequencies of the FE model in SAP2000 and the reference model are compared in table 1. As it is shown, the natural frequencies of the FE model are in reasonable agreement with the theoretical frequencies, as described in [4].

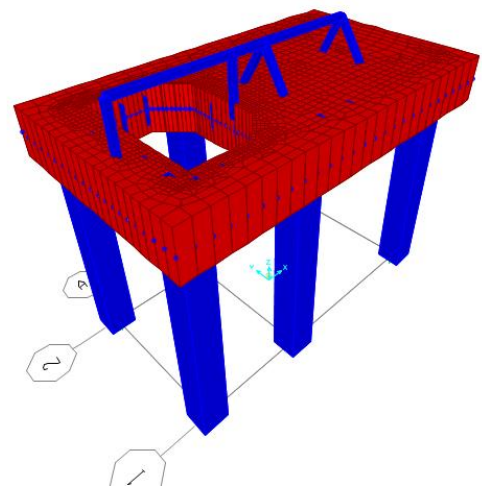


Fig. 1: FE model of turbo generator foundation

Table 1: Natural frequencies of the FE and reference models

Mode	FE model (Hz)	Reference model (Hz)	Difference (%)
1	2.48	2.6646	7
2	2.52	2.7313	8
3	3.20	3.4745	8
4	23.80	23.958	1
5	29.35	30.674	4
6	30.599	31.708	3
7	35.888	37.497	4
8	36.348	38.714	6

### 3.2 System identification using ambient vibration

In this section, a system identification method based on Hilbert transform is employed to identify the damping ratio and the natural frequencies of the TG foundation. The acceleration and displacement responses of the TG foundation under ambient vibration are recorded for 1200 seconds. In this study, it is assumed that data acquisition is carried out during maintenance overhauls. Therefore, during sensor data recording, the TG machine is not in operation and the foundation is solely subjected to ambient excitation, which is modeled as a nonstationary white noise signal. The TG foundation is simulated in Open Sees environment [24].

The structure is subjected to a nonstationary ambient vibration modeled by a product model. The input was assumed to be nonstationary to make the modeling of the ambient excitation more realistic. The stationary input is initially generated as a zero-mean Gaussian white noise signal with a sampling interval of 0.02, a sampling period of 1200 seconds, and a standard deviation of 0.005g. Then, it is multiplied by the amplitude-modulating function  $\Gamma(t) = 4 \times (e^{-0.002t} - e^{-0.004t})$ , as shown in Figure 2. The resulting nonstationary excitation is shown in Figure 3.

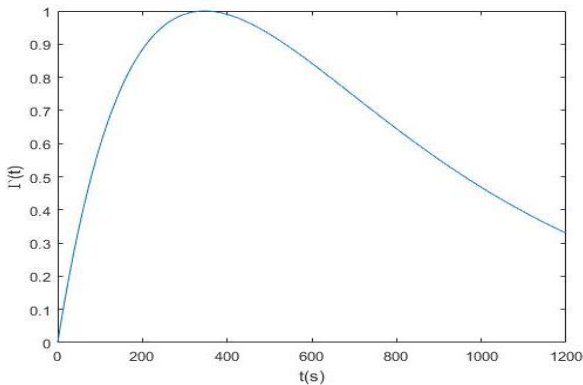


Fig. 1: The amplitude-modulating function

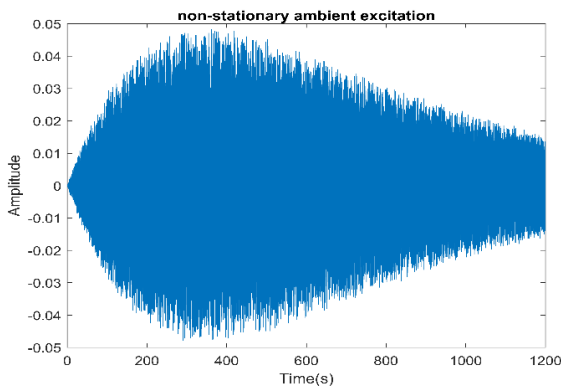
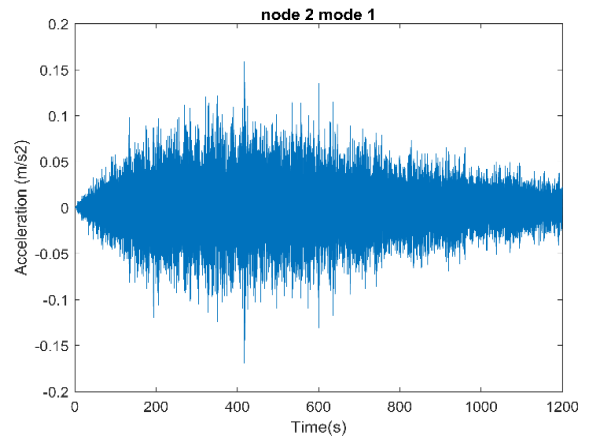


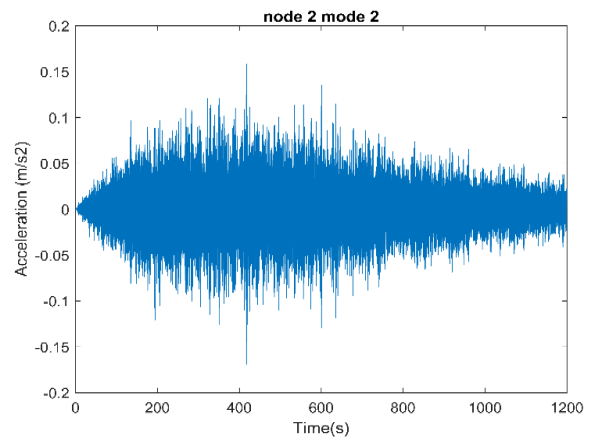
Fig. 2: The nonstationary input vibration

The acceleration responses of the foundation are recorded at a beam-column connection in X, Y, and Z directions and shown in Figure 4.

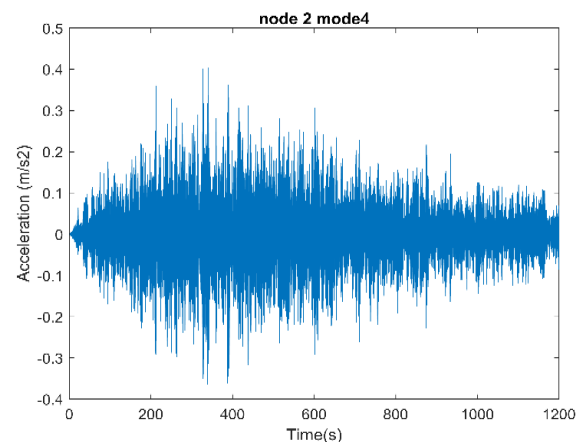
The sensors used for this purpose should have a dynamic range above 120 dB to measure very small vibrations without distorting the signal. The dynamic range of a sensor is the range of signal levels that the sensor can measure. It should be selected based on the range of vibrations that a structure may experience.



(a)



(b)



(c)

Fig. 3: Acceleration response in a) X direction, b) Y direction, and c) Z direction.

### 3.3 natural frequency and damping ratio identification using Hilbert-Huang and AMD transforms

The frequencies and damping ratios can be computed by taking the Hilbert transform of individual oscillations of motion. If the structure is subjected to a nonstationary excitation represented by a product model with a slowly time-varying function, then the nonstationary response time histories could be represented by a product model with the same time-varying function as the excitation,  $f(t)$  [25]. The envelope function  $\Gamma(t)$  can be acquired using the curve-fitting technique. Finally, the nonstationary responses of each DOF are divided into the same envelope function and the resulting signals are the stationary responses of the structure.

Herein, the free vibrations of acceleration responses are determined using the method described in [26], and further decomposed to their intrinsic modes using EMD technique, prior to transformation via Hilbert transform. Figure 5 shows the first five IMFs of the response time history in the X direction. It can be seen that only the first IMF could have a natural frequency of the TG foundation. IMFs 2 to 6 have much smaller amplitudes than that of the first IMF. They are low-energy components with no physical meaning that may result from the sifting process. Thus, these IMFs are considered the residues and could be ignored. For the time-history responses in Y and Z directions, the first three IMFs are represented in Figures 6 and 7.

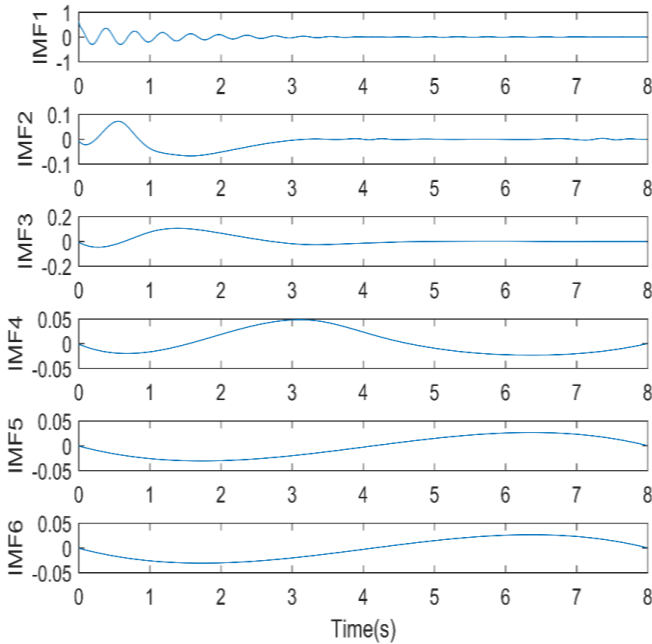


Fig. 4: The IMFs of the acceleration response in X direction

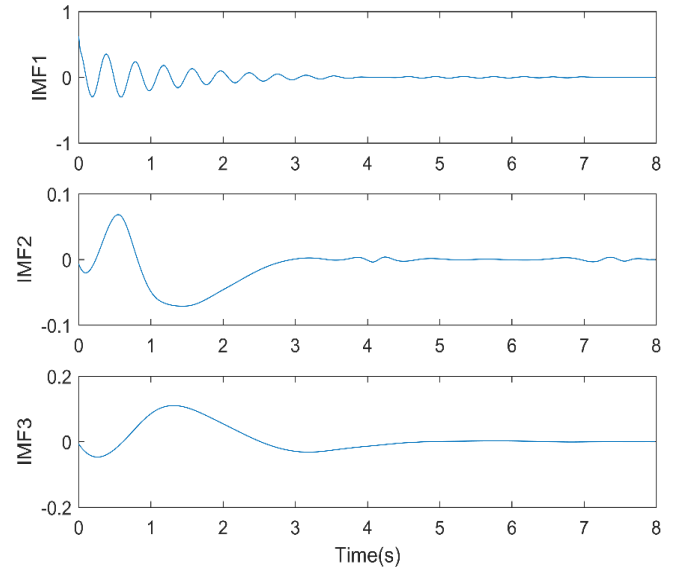


Fig. 5: The IMFs of the acceleration response in Y direction

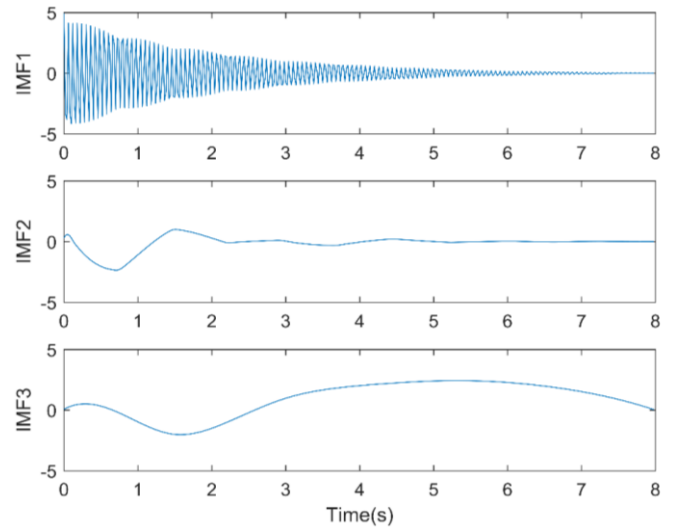


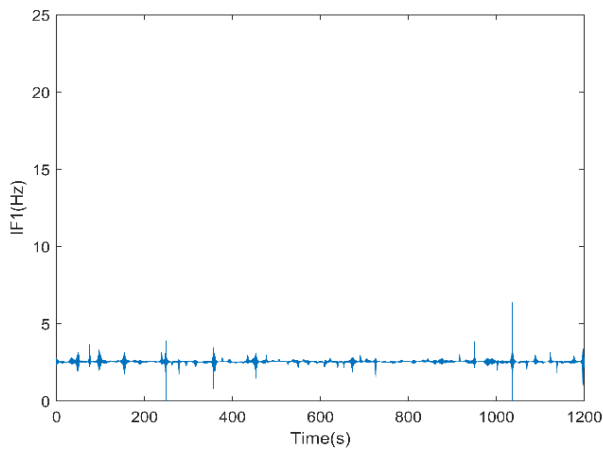
Fig. 6: The IMFs of the acceleration response in Z direction

By taking the Hilbert transform of the first IMFs, the instantaneous frequency and amplitude signals are obtained. As discussed before, the natural frequencies and damping ratios can be extracted using the slopes of the phase-time and log envelope-time signals, respectively. The identified and the theoretical modal properties are compared in Table 2.

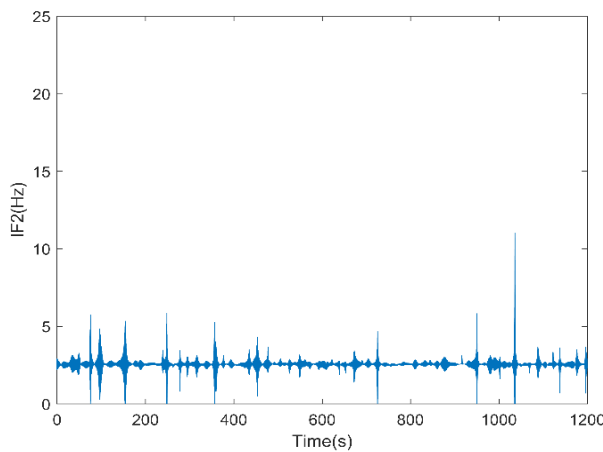
The AMD technique is also used to decompose the acceleration responses to individual vibration signals using multiple bisecting frequencies. The goal is to identify the frequencies of the structure and compare them with EMD results.

The bisecting frequencies were initially obtained using fast Fourier transform, and were considered 2.5 Hz and 3 Hz for the accelerations in X and Y directions, and 23 Hz and 24 Hz for the acceleration in Z direction (Figure 8). The identified and the theoretical frequencies are calculated by the same method used for IMFs and compared in Table 2.

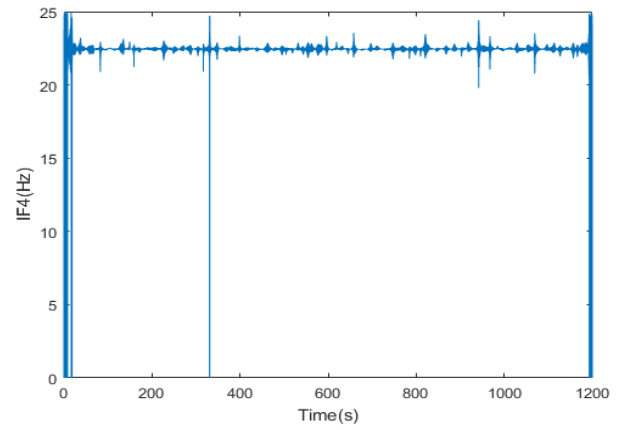
The frequencies of translational modes are correctly identified and the error is less than 5%. However, in EMD method the identified damping ratio in the Z direction does not match the analytical damping ratio.



(a)



(b)



(c)

Fig. 7: The instantaneous frequencies of: (a) first mode (X), (b) second mode (Y), (c) fourth mode (Z)

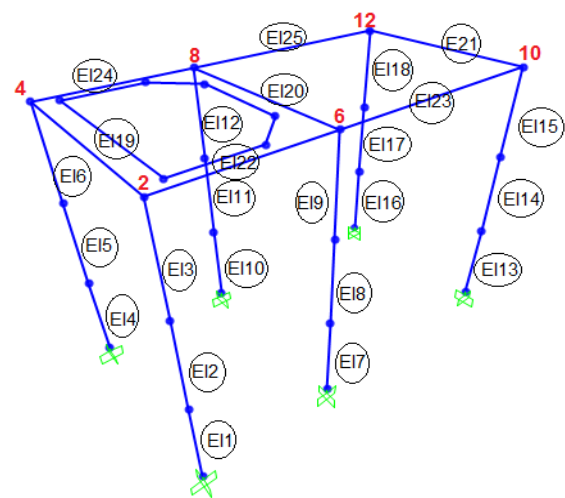


Fig. 9: Frame element numbering

Table 2: Analytical and identified modal properties using EMD and AMD methods

Mode	Analytical frequency (Hz)	Identified frequency-EMD (Hz)	Identified frequency-AMD (Hz)	Analytical damping ratio	Identified Damping Ratio- EMD	Identified Damping Ratio- AMD
1 (X)	2.48	2.38	2.53	0.03	0.03	0.03
2 (Y)	2.52	2.43	2.58	0.03	0.037	0.0305
4 (Z)	23.80	23.32	23.28	0.03	0.005	0.039

### 3.4 Damage detection in TG foundation

In this study, the damage was simulated by reducing the stiffness of different beam and column elements of the TG foundation. The shell element was considered rigid as it is a massive deck with a depth of 1.8 m. Moreover, damage in TG foundations is frequently observed on the beam and column elements.

To evaluate the sensitivity of the method, three different damage scenarios were considered (Table 3). The configuration of the sensors and the damage severities vary in each scenario. The damage severities were selected for three cases of minor damage (0-15 percent of the stiffness is reduced), intermediate damage (15-25 percent of the stiffness is reduced), and severe damage (25-35 percent of the stiffness is reduced).

The reduction factor,  $\alpha$ , was the updating parameter in the GA algorithm, which shows the extent to which the element has been damaged. Moreover, the column elements in the initial FE model were divided into 3 segments (Figure 9). The beams were not divided into smaller beams to keep the number of updating parameters small. Overall, 25 elements were modeled, which means 25 parameters should be updated in the optimization process.

**Table 3:** Different damage scenarios for damage detection

Damage scenario	Damaged elements	Damage severity
S1	2,8, 13,17, 20,	15%
S2	2,3,8,9,15,23	25%
S3	4,16,14,21	35%

In this work, the real-coded genetic algorithm was used for model updating, with all 25 parameters embedded in each chromosome as genes were estimated in a predefined range of [0,1].

To detect the damage, the responses of the intact structure, which is modeled based on design documents, and the identified structure, which is modeled based on ambient data, are used in an optimization process.

### 3.4.1 Objective function

A single-objective genetic algorithm was employed for detecting damage in the TG foundation. The objective function was based on the instantaneous frequencies and amplitudes of the acceleration responses. The sensors were located at nodes 2, 8, and 10 for data acquisition, since at least three time-histories were required to capture sufficient vibration information. The objective function was formulated as:

$$J = J_{\omega 8} + J_{acc2} + J_{acc8} + J_{acc10} \quad (22)$$

Where  $J_{\omega 8}$ ,  $J_{acc2}$ ,  $J_{acc8}$ ,  $J_{acc10}$  are the residuals of instantaneous frequency at node 8, and instantaneous amplitudes at nodes 2, 8, and 10, respectively. The instantaneous properties considered in the J function were extracted from the lower components of the acceleration responses. The residuals were defined as:

$$J_{\omega}(E) = \left\{ \sum_{j=1}^{N_e} \left[ \frac{\omega_j^u(E, t) - \hat{\omega}_j^m(t)}{\hat{\omega}_j^m(t)} \right]^2 \right\} \quad (23)$$

$$J_{acc}(E) = \left\{ \sum_{j=1}^{N_e} \left[ \frac{A_j^u(E, t) - \hat{A}_j^m(t)}{\hat{A}_j^m(t)} \right]^2 \right\} \quad (24)$$

Where E is the updating parameters vector,  $N_e$  is the number of time instants, A is the instantaneous amplitude,

$\omega$  is the instantaneous frequency, u and m denote the parameters of the updated model and the main model, respectively.

In fact, the optimization problem here is a minimization problem, where the sum of aforementioned residuals is minimized through elemental stiffness updating. In this case, the objective function could be considered as a cost function, which should reach a minimum value, also considered as the cost value.

The acceleration responses were recorded for 100 seconds with a sampling interval of 0.02 seconds to reduce the computational time. Furthermore, only 500 out of total 5000 recorded data points, selected from the middle of the signals, were used for the residual optimization, as described in [27].

### 3.4.2 GA parameters and procedure

The population size, maximum number of iterations, crossover and mutation probabilities were set as 80, 40, 0.8, and 0.3, respectively. The algorithm evaluated 3600 solutions through 40 iterations. The number of iterations was determined by the trial-and-error method. After 40 iterations no significant improvements in the estimations were observed, indicating that the cost function did not change remarkably.

Each damage scenario shown in Table 3 is first applied to the analytical model (in Open Sees) by reducing the stiffness of the corresponding elements. The acceleration responses of the FE model under the nonstationary ambient vibration are then obtained and considered as the responses of damaged structure in the genetic algorithm. The same acceleration responses for the intact structure (the FE model with no stiffness reduction) are also obtained.

According to Figure 9, there are 25 frame elements in the FE model which means 25 material models are defined in Open Sees. The stiffness parameters of elements are the updating parameters of the genetic algorithm, defined as genes that are encoded in each chromosome.

For each damage scenario, these parameters are updated by the GA and then adjusted as stiffness parameters in the analytical model to obtain the acceleration responses and compare the instantaneous frequency and acceleration amplitude signals of the updated model with those of the intact model. This procedure is repeated 40 times (number of iterations). The GA evaluates the fitness of the objective function in each iteration. In this case, the discrepancy between the two models shall be minimized. Therefore, the smaller the residuals in equations (27) and (28), the higher the fitness of the solution.

Figure 10 shows the detailed procedure of FE model updating implemented in MATLAB and Open Sees.

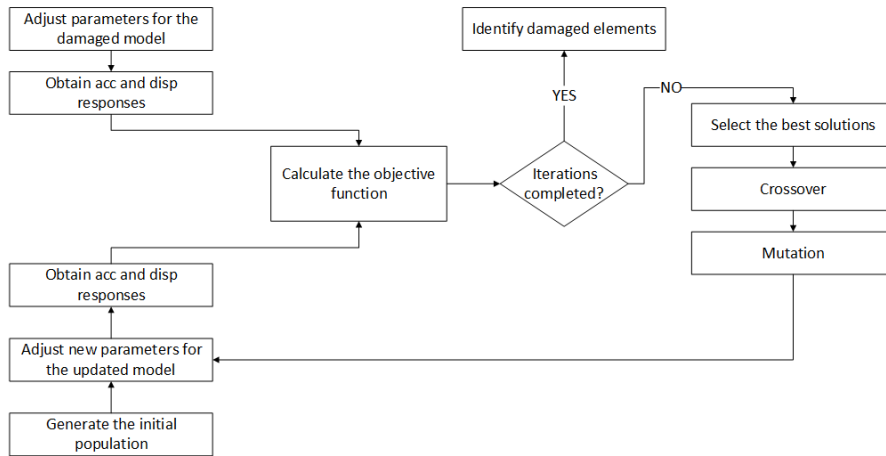


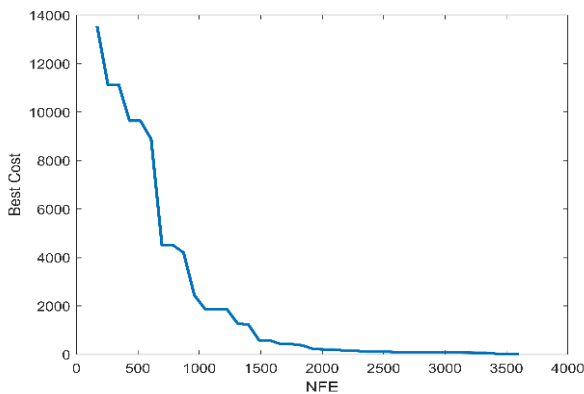
Fig. 10: Detailed procedure of FE model updating

### 3.5 Model updating results

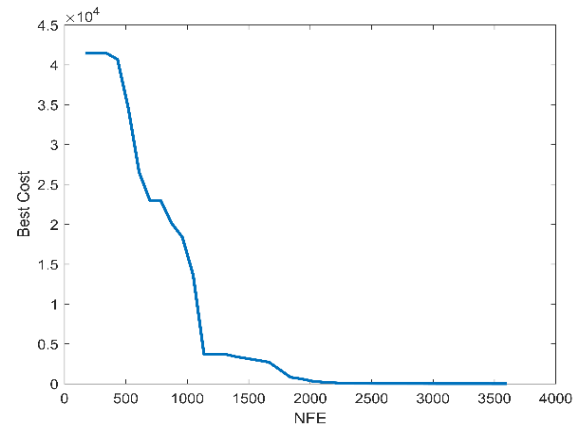
The best cost in each evaluation indicates the minimum value of the objective function. The total number of function evaluations (NFE) is calculated using the equation:

$$NFE = Npop + (Nc + Nm) \times It \tag{29}$$

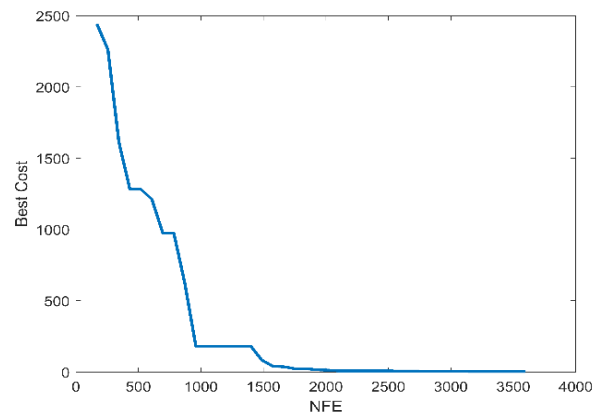
Where Npop, Nc, Nm, and It are the population size, the crossover population, the mutation population, and the number of iterations, respectively. Figure 11 depicts the cost values over the number of evaluations for three damage scenarios. It is seen that as the iterations increase, the cost values decrease. It continues until the cost values reach a point where no more reductions occur and the trend becomes flat. This point is the minimum value of the objective function after 40 iterations and 3600 evaluations. The cost converges to 24, 3.9, and 1.03 for the first, second and third damage scenarios, respectively. The initial cost at each case is large because the algorithm starts with a random initial population and has no prior knowledge about the location or extent of damage. Although the final cost is nonzero, the algorithm’s performance in response estimation is promising.



(a)



(b)



(c)

Fig. 8: Optimization results for a) damage scenario 1, b) damage scenario 2, and c) damage scenario 3

## 4. Results and discussion

The results for the detected damaged elements in each scenario are shown in Figures 12 to 14. In the first scenario, the Young’s moduli in elements 2, 8, 13, 17, and 20 are reduced by 15%. As shown in Figure 12, the locations of

damaged elements are successfully detected. However, the number of incorrect damage locations is considerable. Elements 11, 15, 18, and 23 are false estimations. Some other undamaged elements are wrongly diagnosed with damages, but the extents are below 10%. The extents of detected damaged elements, on the other hand, have 45% errors on average. Overall, the results are not reliable if the damage severities of elements are 15% or less.

In the second case, the elements 2, 3, 8, 9, 15, and 23 are damaged by 25%. As shown in Figure 13, the number of false detections were reduced this time; Only two elements were wrongly diagnosed with severe damages. The damaged elements were localized correctly. In this scenario, the elements 2 and 3 are in the same column. The elements 8 and 9 are also in the same column. The average detected extents of these elements are equal to the real simulated extents.

In the third case, the elements 4, 14, 16, and 21 are damaged to the extend of 35%. In this scenario, only one element is diagnosed with severe damage. As shown in Figure 14, other detected damaged elements have extents below 10%, or agree with the real extents of damages. Elements 4 and 5 are in the same column and can be

considered approximately correct as they reflect the damage in the right column. In this case, the damages are accurately localized, except for the element 19. The extents of detected damages are also close to the real simulated damages.

The results show that the proposed method can effectively detect the presence and location of the damage when the extent of damage is 25% and 35%. For the first damage scenario (15% damage), the results were not sufficiently precise. In this case, 3 out of the total 8 detected damaged elements were wrongly diagnosed.

The estimated extents of damages were close to the real extents for all damaged elements, in the third damage scenario (35% damage). If two elements in the same column are damaged, their locations may be mistaken. However, the method can detect the overall extents correctly. This can be sufficient for the main goal of damage detection and localization in the TG foundation. In the second damage scenario, the damage localization results are satisfactory. The estimations for extents of damages, however, were not as accurate as those in the third damage scenario.

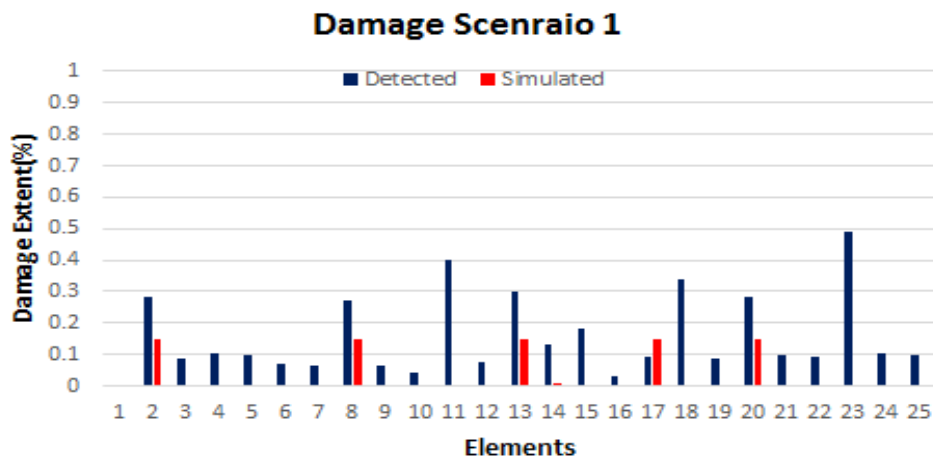


Fig. 9: Damage detection results for damage scenario 1

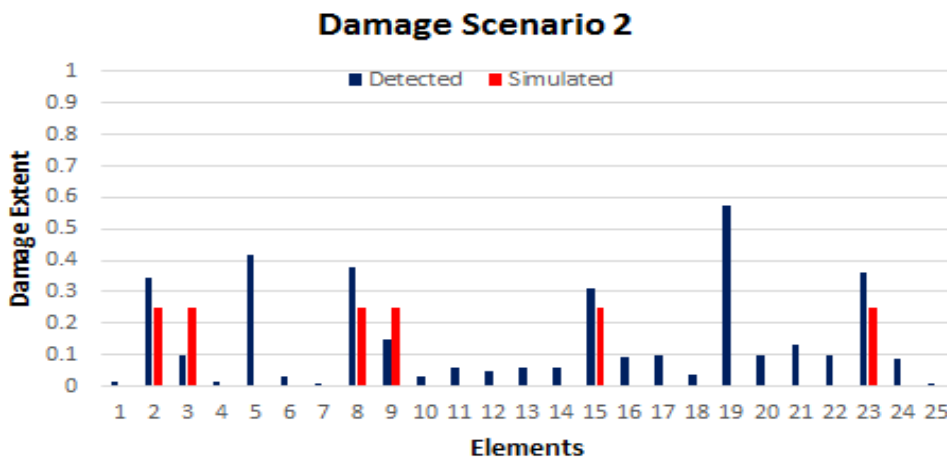


Fig.10 : Damage detection results for damage scenario 2

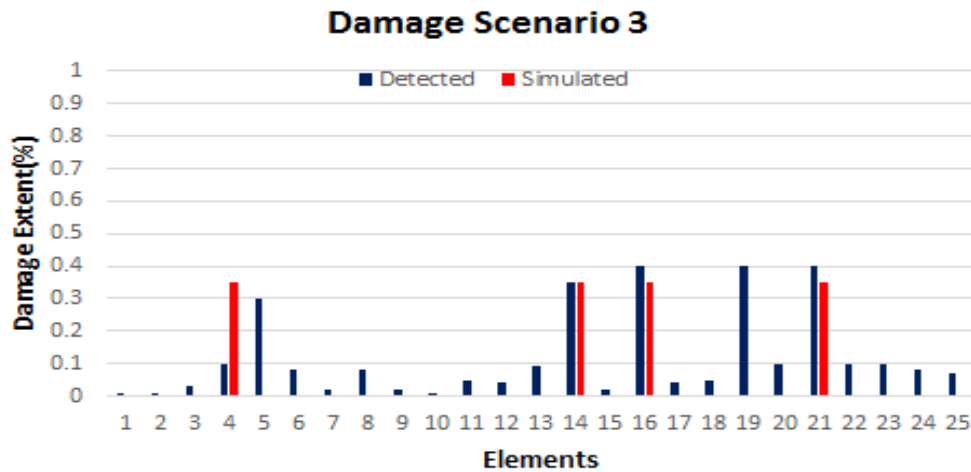


Fig. 14: Damage detection results for damage scenario 3

## 5. Conclusion

In this study, an FE model updating procedure was employed for detecting structural damage in a frame-type TG foundation. The Hilbert-Huang and Analytical mode decomposition methods were used for natural frequency and damping identification of the TG foundation. In the second stage, different damage scenarios were modeled and further detected using model updating methods and genetic algorithm. The objective function was constructed by instantaneous properties of the TG foundation. The concluding remarks are as follows:

- The proposed damage detection method could properly locate the intermediate to severe damages in the 3-D TG foundation (e.g. when more than 20% of the element is damaged). The estimations for the location of damage got better as the severity of damage increases.
- The proposed method could accurately quantify the severe damages (e.g., when the extent of damage is more than 35%).
- At least three sensors are required to capture sufficient vibration data for damage detection. The sensor configuration does not affect the accuracy of the method. This means the method locates the intermediate and severe damages regardless of the damages and sensor locations.
- The proposed method is not useful for detecting minor damages.
- The modal frequencies and damping ratios can be obtained using Hilbert-Huang transform with less than 5% error. For this purpose, the accelerations in all translational degrees of freedom are needed.
- The analytical mode decomposition technique proved to be effective and accurate in natural frequency identification of the 3-D TG foundation, using the acceleration responses in translational modes.

## References

- [1] J.-H. Lee, J.-E. Jung, N.-G. Kim, and B.-H. Song, "Industrial Pipe-Rack Health Monitoring System Based on Reliable-Secure Wireless Sensor Network," *Int. J. Distrib. Sens. Networks*, 2012, doi: 10.1155/2012/641391.
- [2] S. M. C. M. Randiligama, D. P. Thambiratnam, T. H. T. Chan, S. Fawzia, and K. D. Nguyen, "Vibration based damage detection in hyperbolic cooling towers using coupled method," *Eng. Fail. Anal.*, 2021.
- [3] R. Manabe, H. Kawae, K. Ogawa, and M. Matsuura, "Maintenance Management of Turbine Generator Foundation Affected by Alkali-Silica Reaction," *J. Adv. Concr. Technol.*, vol. 14, no. 590–606, 2016.
- [4] K. G. Bhatia, *Foundations for Industrial Machines Handbook for Practising Engineers*. 2008.
- [5] K. Roy, "Structural Damage Identification Using Mode Shape Slope and Curvature," *J. Eng. Mech.*, vol. 143, no. 9, 2017.
- [6] F. Frigui, J. P. Faye, C. Martin, O. Dalverny, F. Peres, and F. Judenherc, "Global methodology for damage detection and localization in civil engineering structures," *Eng. Struct.*, vol. 171, pp. 686–695, 2018.
- [7] H. Zhu, L. Li, and X.-Q. He, "Damage detection method for shear buildings using the changes in the first mode shape slopes," *Comput. Struct.*, vol. 89, pp. 733–743, 2011.
- [8] M. S. Cao, G. G. Sha, Y. F. Gao, and W. Ostachowicz, "Structural damage identification using damping: a compendium of uses and features," *Smart Mater. Struct.*, vol. 26, 2017.
- [9] A. Zare Hosseinzadeh, G. Amiri, Ghodrati, S. A. Seyed Razzaghi, K. Y. Koo, and S. H. Sung, "Structural damage detection using sparse sensors installation by optimization procedure based on the modal flexibility matrix," *J. Sound Vib.*, vol. 381, pp. 65–82, 2016.
- [10] Y.-S. Kim and H.-C. Eun, "Comparison of Damage Detection Methods Depending on FRFs within Specified Frequency Ranges," *Adv. Mater. Sci. Eng.*, 2017, doi: doi.org/10.1155/2017/5821835.

[11] J. Hou, S. Wang, Q. Zhang, and L. Jankowski, "An Improved Objective Function for Modal-Based Damage Identification Using Substructural Virtual Distortion Method," *Appl. Sci.*, vol. 9, no. 5, 2019.

[12] M. M. ABDEL WAHAB, "EFFECT OF MODAL CURVATURES ON DAMAGE DETECTION USING MODEL UPDATING," *Mech. Syst. Signal Process.*, vol. 15, no. 2, pp. 439–445, 2001.

[13] L. Yu and T. Yin, "Damage Identification in Frame Structures Based on FE Model Updating," *J. Vib. Acoust.*, vol. 132, no. 5, 2010.

[14] J. Li and H. Hao, "Substructure damage identification based on wavelet-domain response reconstruction," *Struct. Heal. Monit.*, 2014, doi: 10.1177/1475921714532991.

[15] N. F. Alkayem, M. Cao, Y. Zhang, M. Bayat, and Z. Su, "Structural damage detection using finite element model updating with evolutionary algorithms: a survey," *Neural Comput. Appl.*, pp. 389–411, 2017.

[16] Y.-J. Cha and O. Buyukozturk, "Structural Damage Detection Using Modal Strain Energy and Hybrid Multiobjective Optimization," *Comput. Civ. Infrastruct. Eng.*, vol. 30, pp. 347–358, 2015.

[17] G. Chen and Z. Wang, "A signal decomposition theorem with Hilbert transform and its application to narrowband time series with closely spaced frequency components," *Mech. Syst. Signal Process.*, vol. 28, pp. 258–279, 2012.

[18] Z. Wang and G. Chen, "Analytical mode decomposition with Hilbert transform for modal parameter identification of buildings under ambient vibration," *Eng. Struct.*, vol. 59, pp. 173–184, 2014.

[19] M. Feldman, "Non-linear free vibration analysis using Hilbert transform - I. Free vibration analysis method 'freevib,'" *Mech. Syst. Signal Process.*, vol. 8, no. 2, pp. 119–127, 1994.

[20] M. Feldman, "Time-varying vibration decomposition and analysis based on the Hilbert transform," *J. Sound Vib.*, vol. 295, no. 3–5, pp.

[21] N. E. Huang, Z. Shen, S. R. Long, M. C. Wu, H. H. Shih, and Q. Zheng, "The empirical mode decomposition and the Hilbert spectrum for nonlinear and non-stationary time series analysis," in *Proceedings of The Royal Society A*, 1998, pp. 903–995.

[22] S. Hassiotis and G. D. Jeong, "Identification of stiffness reductions using natural frequencies," *J. Eng. Mech.*, vol. 121, no. 10, pp. 1106–1113, 1995.

[23] M. Ratcliffe and N. Lieven, "An improved method for parameter selection in finite element model updating," *Aeronaut. J.*, vol. 102, no. 1016, pp. 321–329, 1968.

[24] P. Earthquake and B. Engineering Research Center (PEER), University of California, "OpenSees, 'Open System for Earthquake Engineering Simulation,'" 2008. .

[25] C.-S. Lin and D.-Y. Chiang, "A modified random decrement technique for modal identification from nonstationary ambient response data only," *J. Mech. Sci. Technol.*, vol. 26, no. 6, pp. 1687–1696, 2012.

[26] G. H. James, T. G. Carne, and J. P. Lauffer, "The Natural

Excitation Technique (NExT) for Modal Parameter Extraction From Operating Wind Turbines," *SAND92-1666. UC-261, Sandia Natl. Lab.*, 1993.

[27] W. Zuo-Cai, Y. Xin, and W.-X. Ren, "Nonlinear structural model updating based on instantaneous frequencies and amplitudes of the decomposed dynamic responses," *Eng. Struct.*, vol. 100, pp. 189–200, 2015.



This article is an open-access article distributed under the terms and conditions of the Creative Commons Attribution (CC-BY) license.